Electronic Supporting Information For:

In Vivo Imaging Using Polymeric Nanoparticles Stained With Near-Infrared Chemiluminescent and Fluorescent Squaraine Catenane Endoperoxide

Jung-Jae Lee, Alexander G. White, Douglas R. Rice, and Bradley D. Smith*
Department of Chemistry and Biochemistry, University of Notre Dame, Notre Dame, IN 46556
*email: smith.115@nd.edu

Contents

1. Synthesis of SCEP by Photoxidation of SC

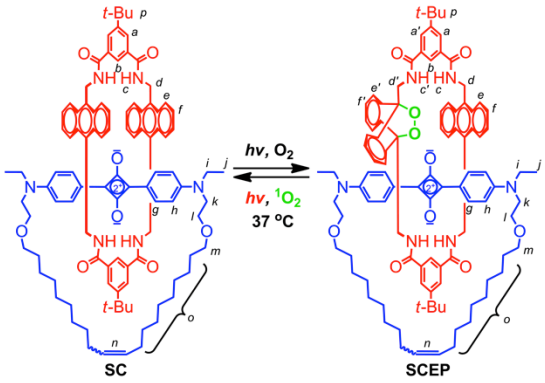

The known **SC**[S1] (15 mg) was dissolved in $CDCl_3$ (0.6 mL) and added to a standard NMR tube. The uncapped tube was placed 10 cm in front of a filtered (long-pass, 520 nm) 150 W Xenon lamp and irradiated for two hours with exposure to air. Complete conversion to **SCEP** was confirmed by ^{1}H NMR spectroscopy (Figure S1). The solvent was removed under reduced pressure at ice-bath temperature to give pure **SCEP**, which was stored as a solid or organic solution at temperatures below 0 °C until needed. (Safety note: organic endoperoxides with high oxygen content are potentially shock-sensitive materials and should be handled in small portions.) ^{1}H NMR (500 MHz; $CDCl_3$) 9.42 (s, 2H), 8.74 (bs, 2H), 8.65 (s, 2H), 8.50 (s, 2H), 7.86 (dd, *J* = 6.5, 3.0, 4H), 7.30 (bs, 2H), 7.23 (d, *J* = 9.0, 4H), 7.15 (dd, *J* = 5.5, 3.5, 4H), 6.84 (dd, *J* = 6.5, 3.0, 4H), 6.49 (dd, *J* = 5.5, 3.0, 4H), 6.23 (d, *J* = 9.5, 4H), 5.44 (d, *J* = 9.5, 4H), 4.28 (d, *J* = 4.5, 4H), 3.77 (bs, 4H), 3.68 (bs, 6H), 3.64 (t, *J* = 7.2 Hz, 4H), 3.55 (t, *J* = 6.6 Hz, 4H), 1.57 (s, 18H), 1.66-0.40 (m, 38H); Cycloreversion prevents acquisition of clean ^{13}C NMR spectrum. MS(ESI): calcd. for $C_{100}H_{117}N_6O_{10}$ $(M+H)^+$ 1561.8826, found 1561.8836. Photophysical properties in chloroform (5.0 μM), λ_{abs} 665 nm, λ_{em} 696 nm, log ε 5.1, Φ_f 0.40.

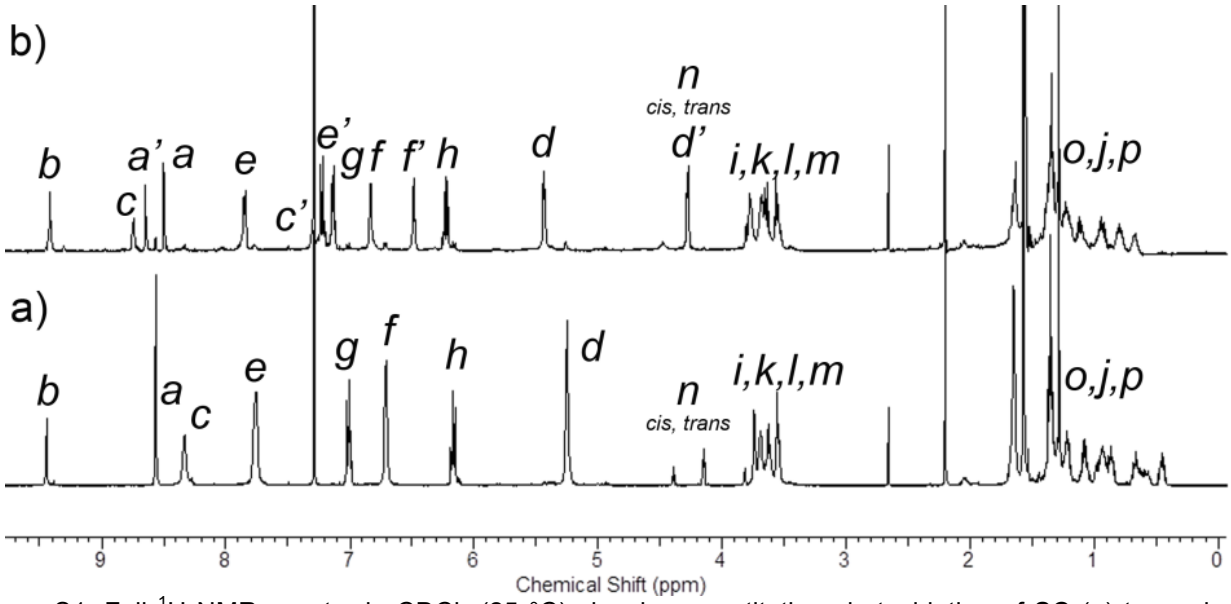

Figure S1. Full ^{1}H NMR spectra in $CDCl_3$ (25 °C) showing quantitative photoxidation of **SC** (a) to produce **SCEP** (b), achieved by irradiating an NMR tube with red light for two hours in the presence of air. The atom assignments are based on through-bond and through-space connectivities determined by multidimensional NMR methods and also the close homology of chemical shifts with the established structure of **SREP**.[S2] The above spectra of **SC** and **SCEP** exhibit symmetrical and coalesced signal patterns that imply rapid circumrotation of one interlocked macrocycle relative to the other. For more discussion of the molecular dynamics, see reference S1.

2. SCEP Cycloreversion to SC in Organic Solution

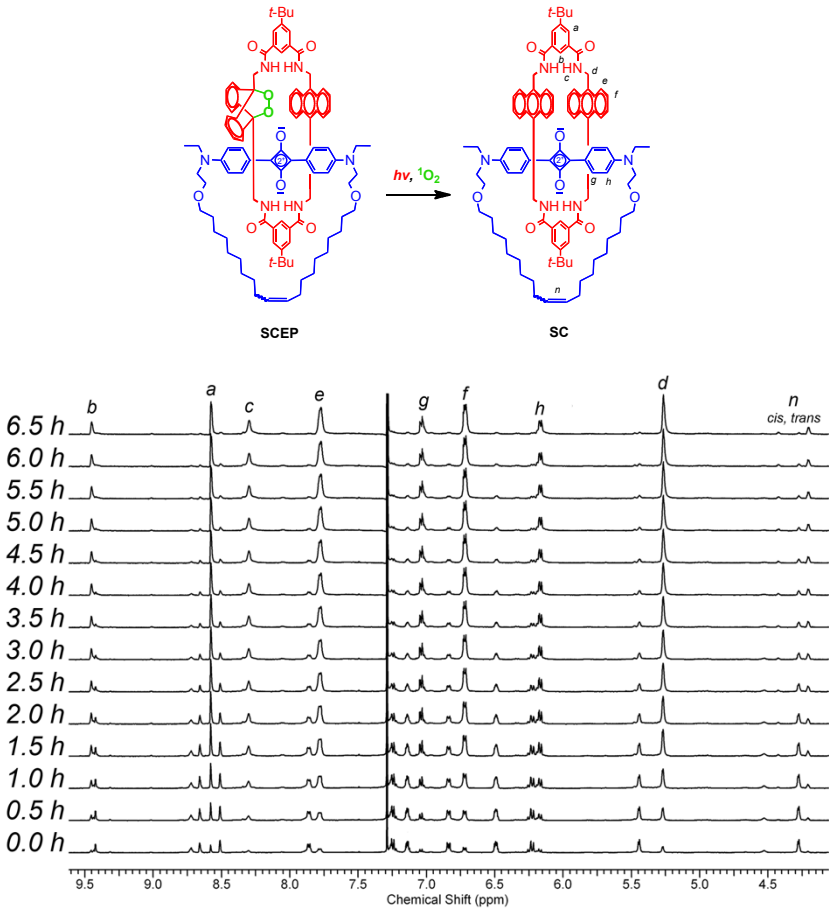

Figure S2. ^{1}H NMR spectra showing complete cycloreversion of **SCEP** to **SC** at 38 °C in $C_2D_2Cl_4$. The starting situation for this specific sample at time 0 h was ~80% **SCEP** and 20% **SC**.

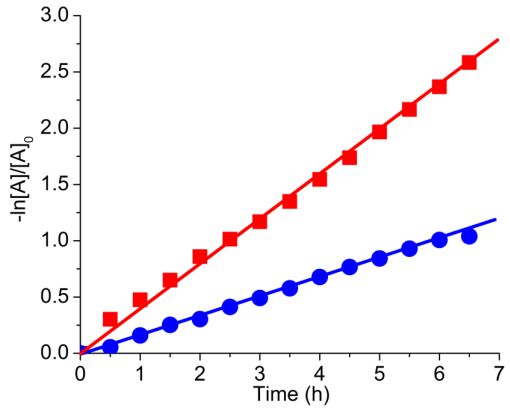

Figure S3. First order kinetic plots for cycloreversion of **SREP** (blue) and **SCEP** (red) at 38 °C in $C_2D_2Cl_4$.

3. Chemical Trapping of Released Singlet Oxygen[S2,S3]

A solution of **SC** (3.0 mM) in $CDCl_3$ was irradiated and converted into **SCEP**. A 30-fold excess (90 mM) of 2,3-dimethyl-2-butene was added to the solution and the sample was maintained at 38 ˚C in the dark. After 18 h, the cycloreversion of **SCEP** back to **SC** was complete and a ^{1}H NMR spectrum was acquired with simultaneous saturation of the large signal at 1.8 ppm due to unreacted 2,3-dimethyl-2-butene. The two olefin proton signals for the singlet oxygen trapped product, 2,3,3-trimethylbutene-3-hydroperoxide, **S1,** appear in the open window of 4.9-5.1 ppm. Comparison of the **S1** peak integrals with regenerated **SC** signals showed that 60±5% of the released oxygen was singlet oxygen and trapped as **S1** (Figure S4). Previously reported trapping experiments with **SREP** showed that that 64±10% of the released oxygen was singlet oxygen.[S2]

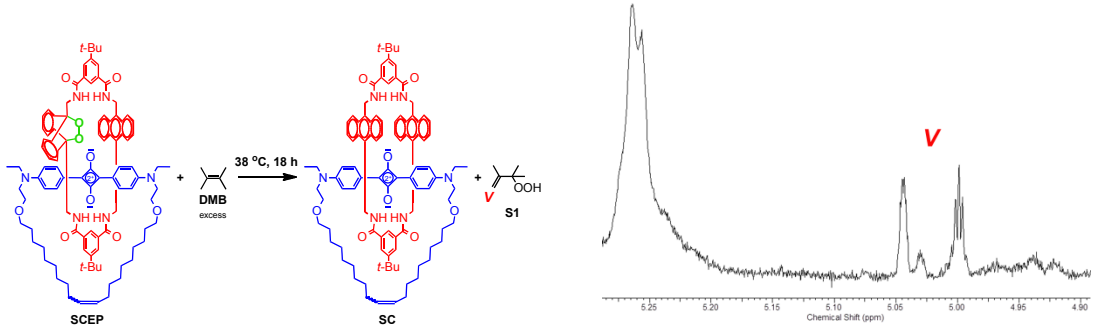

Figure S4. (*left*) The singlet oxygen that is released by cycloreversion of **SCEP** is trapped by undergoing an ene reaction with excess 2,3-dimethyl-2-butene (DMB) to produce 2,3,3-trimethylbutene-3-hydroperoxide, **S1**, which was quantified by ^{1}H NMR spectroscopy. (*right*) Expanded ^{1}H NMR spectrum showing the two olefin proton signals for **S1** at 5.00 and 5.04 ppm.

4. Preparation and Characterization of Dye-Stained Polysyrene Nanoparticles

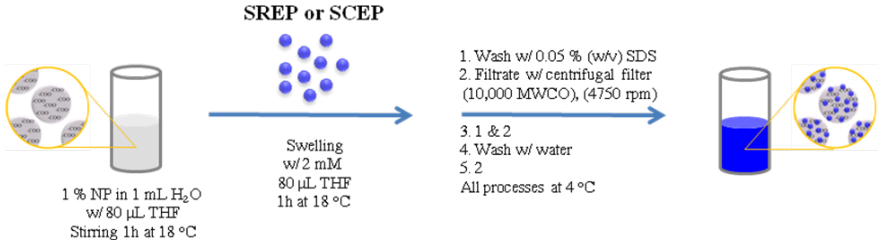

Figure S5. Preparation of dye-doped carboxylate-functionalized polystyrene nanoparticles.[S4]

An aliquot of tetrahydrofuran (THF, 80 µL) was added to a 1.0 mL aqueous suspension of 1.0 % (w/v) carboxylate- functionalized polystyrene particles (20 nm from Invitrogen). The mixture was stirred for 1 h at 18 °C, to induce particle swelling, followed by addition of a solution of **SCEP** or **SREP** in cold THF (80 µL, 2.0 mM). After stirring for an additional 1 h at 18 °C, the mixture was centrifuged at 7,000 rpm. for 2 min. The blue supernatant was discarded, and the blue pellet containing the stained particles was transferred to a centrifugal filter (10,000 MWCO from Millipore) and then washed twice by adding 1.0 mL of aqueous sodium dodecyl sulfate (0.05 % w/v) followed by centrifugation at 4750 rpm. The particles were finally washed with water and resuspended in water (200 µL). Dye loadings, determined by measuring the absorbance of the stained nanoparticles in DMF solution, showed nearly identical loadings of ~14 **SCEP** or **SREP** molecules per single 20 nm nanoparticle.

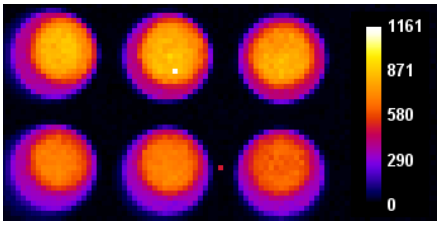

SREP-microparticles
(0.9 μm carboxylate-functionalized polystyrene)

SCEP-microparticles
(0.9 μm carboxylate-functionalized polystyrene)

Figure S6a. Chemiluminescence pixel intensity images of six vials viewed from above. The top three vials contain **SREP**-microparticles (0.9 μm carboxylate-functionalized polystyrene) and the bottom three vials contain **SCEP**-microparticles (0.9 μm carboxylate-functionalized polystyrene). The emission intensities from these micron-sized particles is essentially equal.

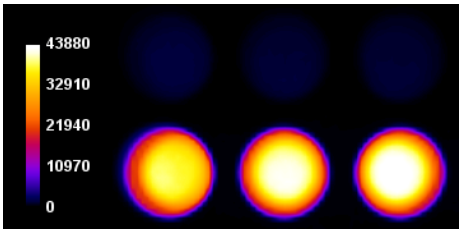

SREP-nanoparticles
(20 nm carboxylate-functionalized polystyrene)

SCEP-nanoparticles
(20 nm carboxylate-functionalized polystyrene)

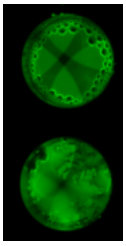

Figure S6b. (*left*) Chemiluminescence pixel intensity images of six vials viewed from above. The top three vials contain **SREP**-nanoparticles (20 nm carboxylate-functionalized polystyrene) and the bottom three vials contain **SCEP**-nanoparticles (20 nm carboxylate-functionalized polystyrene). The emission intensities from the **SCEP**-nanoparticles is about 30 times more intense. (*right*) Fluorescence pixel intensity images of two of the vials containing **SCEP** or **SREP** nanoparticles confirms that the dye loading is about equal in each case.

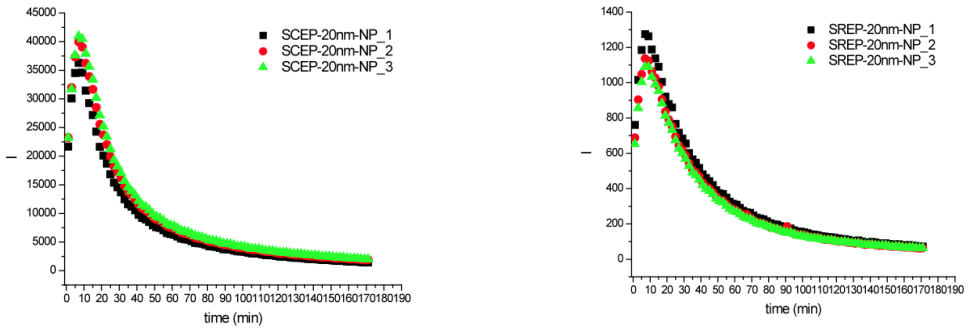

Figure S6c. Decay of the chemiluminescence pixel intensity images in Figure S6b. The y-axis shows chemiluminescent intensity for **SCEP**-nanoparticles is about thirty times brighter than **SREP**-nanoparticles, however, the chemiluminescence decay half-lives are very similar.

5. Integrity of Dye-Stained Polysytrene Nanoparticles

The integrity of the dye-stained nanoparticles under physiological conditions was evaluated by in vitro experiments that incubated the particles with red blood cells and looked for dye transfer to the cell membranes.[S5] The unreactive **SC** was used as the dye for this study. The dye is lipophilic, and as described below, free **SC** was readily removed from aqueous solution by the blood cells. Comparative experiments with **SC**-stained nanoparticles showed essentially no **SC** transfer to the blood cells during a 45 min incubation period. The following experimental procedure was used.

Two stock solutions were prepared. One contained free **SC** (100 μM) in a 1:9 mixture of DMSO:PBA (Dulbecco's phosphate buffered saline, Sigma D5773). The other was **SC**-stained nanoparticles (20 nm carboxylate-functionalized polystyrene particles prepared as above) in PBA with an overall concentration of 100 μM **SC** trapped within 0.5% (w/v) nanoparticles. Separate aliquots from each stock solution (100 μL) were added to separate vials containing either (a) COULTER® 4C®-ES red blood cells (~10^8 cells) in PBA, or (b) pure PBA, and each vial was incubated for at 37 ˚C for 45 minutes. Following incubation, each sample was centrifuged at 800 RCF for 10 min and then photographed (Figure S7). An aliquot of the supernatant (100 μL) from each sample was removed and mixed with 1.9 mL PBA solution in a quartz cuvette. A fluorescence spectrum was acquired (Excitation: 650 nm, Emission: 665 – 750 nm, 22 ˚C), and comparisons of the emission maxima showed that the blood cells removed >60% of the free **SC**, but <10% of the **SC** signal from the **SC**-stained nanoparticles (Figure S8).

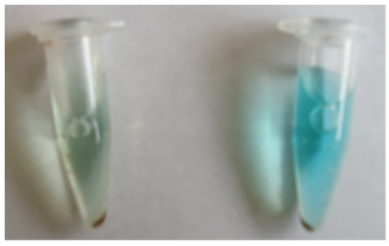

Figure S7. Tubes containing free **SC** (left) and **SC**-stained nanoparticles (right) after 45 min incubation with red blood cells and pelleting of the cells by centrifugation. The cells extracted most of the blue-colored **SC** from the solution but not the **SC**-stained nanoparticles

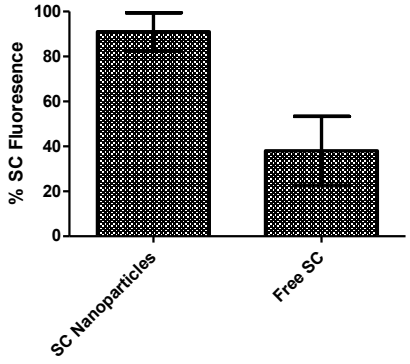

Figure S8. Decrease in **SC** fluorescence intensity at 695 nm in the supernatant due to 45 min incubation of free **SC** or **SC**-stained nanoparticles with red blood cells. Errors bars are standard deviation over three experiments.

6. Chemiluminescence and Fluorescence Imaging

All optical imaging was performed on a Xenogen IVIS® Lumina imaging system (Caliper Life Sciences, Alameda, CA) with a thermoelectrically cooled CCD camera. Vials containing solutions were placed on a heated stage set to 40 °C and imaged with a field-of-view of 5.0 cm^2.

Animal Imaging. Animal care and handling procedures were approved by the Notre Dame Institutional Advisory Care and Use Committee. Nude athymic mice (strain NCr Foxn1^{nu}) were purchased and housed with no special requirements. The animals were anesthetized by inhalation of oxygen gas containing 2.5 % isoflurane, delivered at a flow rate of 2 L/min (Butler, Dublin, OH) before intravenous injection of nanoparticles, and they remained under isoflurane anesthesia throughout the subsequent period of whole-body imaging. Anesthetic action was confirmed by foot pinch test and the animals were monitored to ensure that spontaneous respiration was maintained during the imaging. Nanoparticle dosing was achieved by placing the anesthetized mice on a warming pad, stroking the tail from base to tip multiple times to induce blood vessel dilation, and injecting a 100 µL aqueous dispersion of nanoparticles (loaded with 55 nmol of dye), at a steady rate over 3-5 s, into the tail vein using a 29 gauge syringe. Chemiluminescence images were acquired for 300 s with 8 x 8 binning, no light filtration, a field-of-view of 10 cm^2 and the lens aperture fully open. Fluorescence images were acquired for 5.0 s with 2 x 2 binning, Cy5.5 dichroic filter set (ex: 630 ± 25 nm, em: 730 ± 35 nm), F_{stop} setting of 2. Machine control was performed using Living Image® software (v. 3.0). The pixel intensity maps were analyzed using ImageJ (http://rsb.info.nih.gov/ij) by first subtracting the background using the rolling ball method (radius 500 pixels). A region-of-interest was drawn free-hand around the Target (T) or Background (B) and the software calculated mean pixel intensity (MPI) within the region.

Biodistribution analysis. Following whole-body imaging, the anesthetized mice were euthanized via cervical dislocation, and the dissected organs were placed on low reflectance paper and optical images were acquired as described above. It was assumed that the intensity of near-infrared fluorescence from each organ was proportional to the concentration of nanoparticle probe in the organ. MPI for each organ was measured by region-of-interest analysis using the ImageJ program.

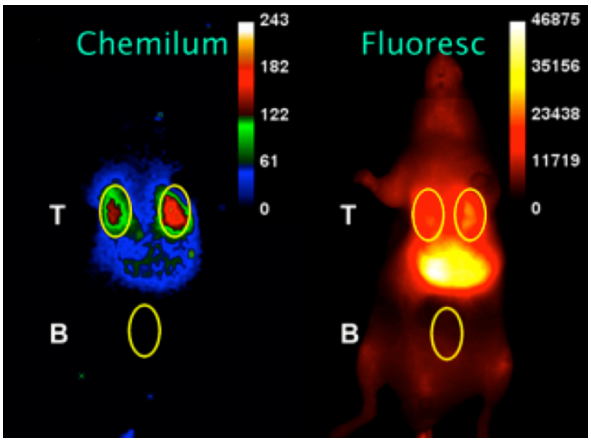

	Chemiluminescence		Fluorescence	
Region	Target MPI	TBR	Target MPI	TBR
L Lung	124	5.7	16592	2.9
R Lung	144	6.6	15602	2.7
Liver	84	3.8	30847	5.4

Figure S9. (*left*) Chemiluminescence and fluorescence pixel intensity images from article Figure 4 showing ventral view of a living mouse (strain NCr Foxn1^{nu}) that had been anesthetized with isoflurane for 30 mins before tail vein injection of **SCEP**-nanoparticles, and imaged about 10 mins later. The oval shapes designate the lung target (T) and non-target background (B) regions. (*right*) Region-of-interest analysis of the chemiluminescence image shows the average Target-to-Background Ratio (TBR) for each lung is 6.2, whereas the fluorescence image shows the average TBR for each lung is 2.8. Furthermore, the average ratio of Lung-to-Liver MPI values is 1.6 for the chemiluminescence image and 0.5 for fluorescence image. The ex vivo imaging data in Figure S10 shows that the actual average ratio of Lung-to-Liver MPI values is 2.2, proving that the in vivo fluorescence image is highly misleading.

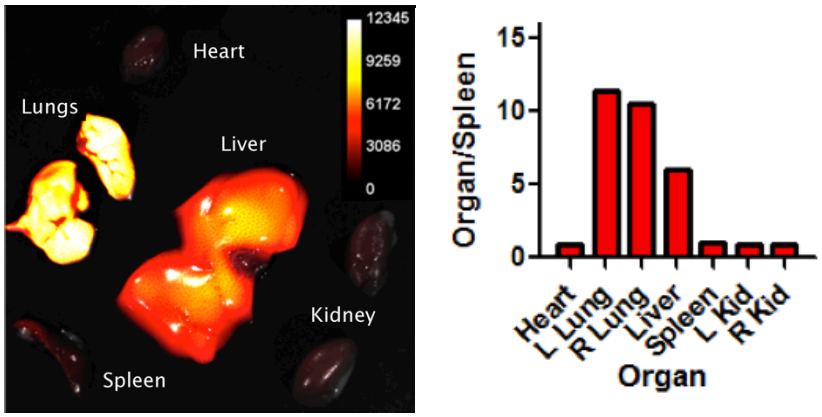

Figure S10**.** (*left*) Fluorescence imaging of excised organs from the mouse in Figure S9, showing biodistribution of **SCEP**-nanoparticles. (*right*) Graphical representation of the region-of-interest analysis of mean pixel intensities (MPI) for each organ relative to the Spleen. The average ratio of Lung-to-Liver MPI values is 2.2.

Histology. The lungs were fixed in formalin overnight, then cut into histological sections and mounted on standard glass microscope slides. Samples were viewed on a Nikon TE-2000 U epifluorescence microscope equipped with a Photometrics 512 B black and white digital camera. Bright field images were acquired for 100 ms using no light filtration. The fluorescence emission of SCEP-nanoparticles was detected using acquisition times of 100 ms and a Cy5 filter set (exciter: HQ620/60X, dichroic: 660LP, emitter: HQ700/75m). Data was collected using a 10x objective (100x total magnification), 60x objective (600x total magnification), and 100x objective (1000x total magnification). Images were evaluated and organized using the ImageJ program and Adobe Photoshop (v 7.0).

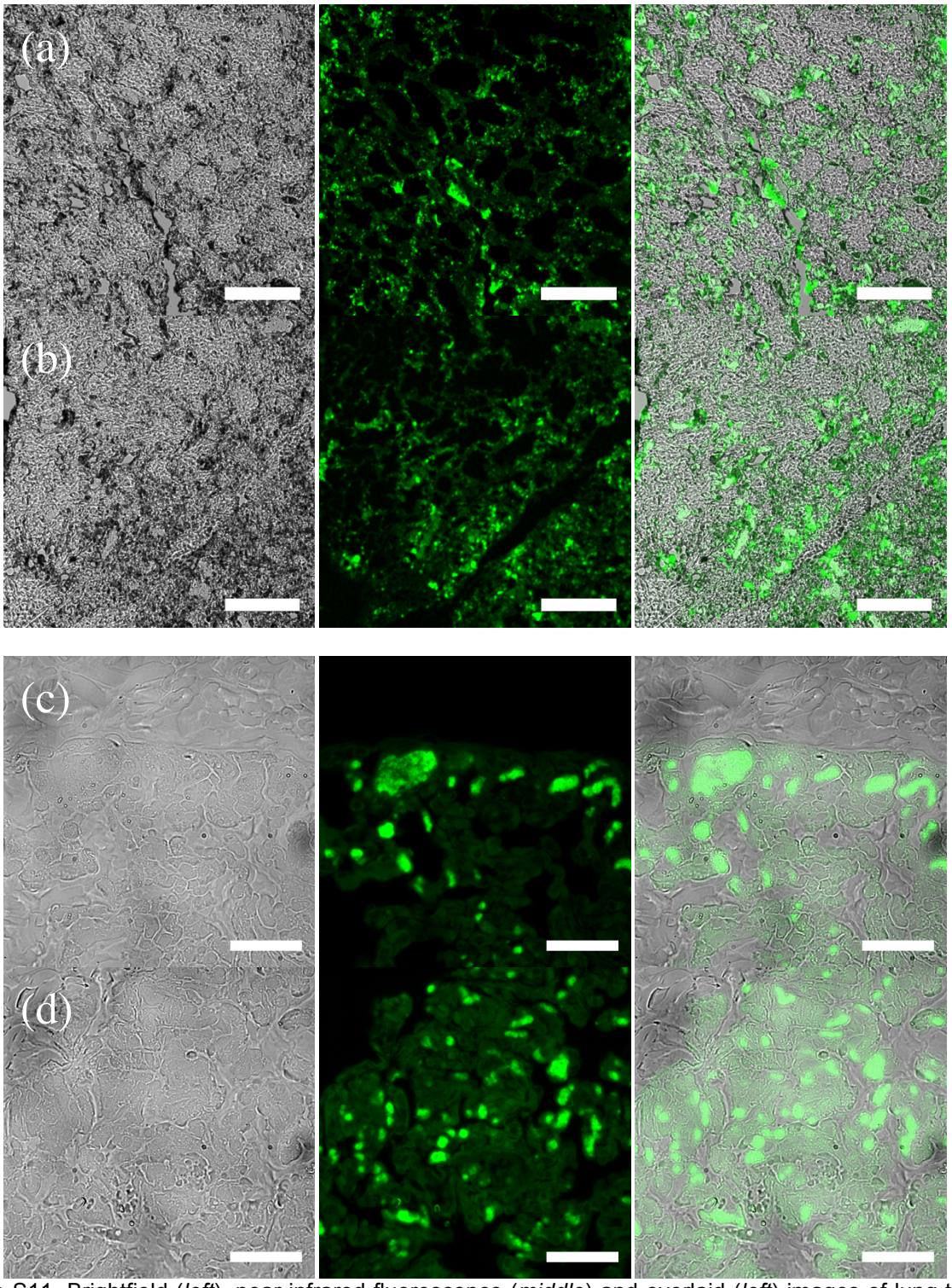

Figure S11. Brightfield (*left*), near-infrared fluorescence (*middle*) and overlaid (*left*) images of lung tissue histology sections taken from the mice that were treated with **SCEP**-nanoparticles. Image rows (a) and (b) were acquired at 100x total magnification. Scale bar = 200 μm. Images (b) and (c) were acquired at 600x total magnification. Scale bar = 30 μm.

[S1] J. -J. Lee, J. M. Baumes, R. D. Connell, A. Oliver and B. D. Smith, *Chem. Commun.,* 2011, **47**, 7188.
[S2] J. M. Baumes, J. J. Gassensmith, J. Giblin, J.-J. Lee, A. G. White, W. J. Culligan, W. M. Leevy, M. Kuno and B. D. Smith, *Nature Chem.,* 2010, **2**, 1025.
[S3] M. Matsumoto,M. Yamada and N. Watanabe, N., *Chem. Commun.,* 2005, 483-485.
[S4] A. B. Descalzo, H. -J. Xu, Z. -L. Xue, K. Hoffmann, Z. Shen, M. G. Weller, X. -Z. You and K. Rurack, *Org. Lett.*, 2008, **10**, 1581.
[S5] P. Andreozzi, C. Martinelli, R. P. Carney, T. M. Carney and F. Stellacci, *Mol. Pharmaceut.* 2012, doi: 10.1021/mp300530c